Hindawi
Advances in Materials Science and Engineering
Volume 2020, Article ID 1921960, 10 pages
https://doi.org/10.1155/2020/1921960

Research Article

Antiexplosion Performance of Engineered Cementitious Composite Explosion-Proof Wall

Guoliang Yang,[1,2] Wenjia Huang,[1] and Shuai Feng[1]

[1]*School of Mechanics and Civil Engineering, China University of Mining and Technology (Beijing), Beijing 100083, China*
[2]*State Key Laboratory of Explosion Science and Technonogy, Beijing, China*

Correspondence should be addressed to Wenjia Huang; sqt1700602041@student.cumtb.edu.cn

Received 28 June 2019; Revised 6 November 2019; Accepted 28 December 2019; Published 20 March 2020

Academic Editor: María Criado

The antiexplosion performance of an explosion-proof wall made of engineered cementitious composite was studied, using small-scale explosion-proof walls made of different materials and sizes that were subjected to on-site blasting. The dynamic responses of these walls were evaluated under blast loading using overpressure test system, digital image correlation (DIC) full-field strain testing, and high-speed photography recording of the crushing process. Analysis of the results of the overpressure and strain tests revealed the effect of the wall height on the overpressure behind the wall. Increasing the height of the explosion-proof wall can improve the protection ratio of the wall by more than 2%. The variation of full-field strain of different materials at the same burst ratio was obtained. The engineered cementitious composite explosion-proof wall was obviously superior to that of ordinary concrete in strain control on the back-explosion surface. These theoretical results provide references for the design of explosion-proof walls.

1. Introduction

Under the action of a dynamic load, especially an explosion impact load, damage of explosion-proof walls is a complex problem, involving the diffraction law of shock-wave overpressure, analysis of the effects of detonation and energy absorption, the influence of structure and materials of the explosion-proof wall on the explosion response, and the scale effect of the test, amongst other considerations. These aspects of research are currently receiving considerable global attention, with the aim of guiding the practice, which is very important for engineering projects, and provide guidance and basis for some aspects of this paper.

In recent years, many scholars have carried out research on the structure and materials of explosion-proof walls using field experiments and digital simulation. In terms of structure and donation, Xu and Lu [1] simulated the delamination of reinforced concrete slabs under different equivalent explosive loads and provided spallation criteria under different spallation conditions. Zhang and Zhang [2] used two-dimensional (2D) mapping of a three-dimensional (3D) mesh simulation for modeling and simulation of a rapidly assembled explosion-proof wall to show that this could be regarded as a rigid explosion-proof wall. The simulated variables were the height of the wall, the proportional explosion distance, and the position of the explosive. The distributions of overpressure along and behind the wall were obtained. Shao and Zhao [3], using LS-DYNA software, analyzed the influence of TNT burst distance, explosive charge, and wall thickness on wall circulation overpressure. Zhang [4] obtained pressure–time curves at different heights in front of and behind an explosion-proof wall using pressure-sensor technology. The change of overpressure of the explosion surface along the wall height was obtained, and a relationship between the back-flow circulation overpressure and the distance from the back-explosion surface was proposed. Ma and Zhao [5] verified the accuracy of finite-element numerical simulation by comparing empirical formulas and calculating the shock-wave resistance of four different types of special-shaped explosion-proof walls under the same explosion conditions.

As for materials, Willauer et al. [6] experimentally compared the impact of a trinitrotoluene (TNT) underwater explosion on wall overpressure and the impulse of an indoor shock wave. Rose et al. [7], using the explosion similarity rate, established a one-tenth-scale riot wall model to study the weakening effect of explosion walls of different materials on an explosion shock wave. Scherbatiuk et al. [8] verified the impact and displacement–time curves of a sand-filled blast wall by establishing a numerical simulation model. Maalej and Zhang [9] experimentally proved that an engineered cementitious composite (ECC) board subjected to high-speed projectile impact experienced low damage, good integrity, multi-slit distribution cracking, and strong energy dissipation. Zhang and Xia [10] used one-dimensional stress-wave theory as the theoretical basis of stress-wave attenuation to calculate the detonation energy-absorption effect of polyurethane, concrete, and aluminum when clamped to a steel plate. Nian and Zhang [11] analyzed the propagation and distribution of transmitted and diffracted shock waves on a flexible wall. Differences in the pressure flow field between the flexible explosion-proof wall and a rigid explosion-proof wall were compared. Zhang and Nian [12] simulated the behavior of TNT explosives under three working conditions: without an explosion-proof wall, with a water-body explosion-proof wall, and with a concrete explosion-proof wall. The time-history curve of energy conversion was obtained for the three materials and it was found that the water-body explosion-proof wall, which relied on its own mass and inertia, could have the same wave-eliminating effect as the concrete explosion-proof wall. In addition, the literature [13–17] also studies the destructive mode and dynamic response of explosion-proof walls.

Although previous studies have shown that explosion-proof wall structures and materials have an impact on antiexplosion performance, the differences in the height and materials under the same burst ratio do not explain the qualitative analysis of the energy-absorption effect of an explosion-proof wall. Although concrete is widely used as a building material, there are still deficiencies in its application for infrastructure construction, such as brittle failure under extreme loads. Impact and crushing under blast loading are related to its poor tensile strength. Engineered cementitious composites (ECC) exhibit high ductility under both tensile and shear loads and have great advantages in enhancing safety, durability, and sustainability of structures. Studying the application of ECC materials in the field of explosion-proof walls and antiexplosion engineering has great significance. So we test the pressure and strain of an explosion-proof wall of specific size and material form and revealed that the ECC explosion-proof walls which are higher have better and energy-absorption effect.

2. Experimental

2.1. Experimental Design. According to the principle-of-similarity ratio, nine explosion-proof walls were prepared. The antiexplosion properties of plain concrete, an ECC material, and reinforced concrete were compared and analyzed. Their dimensions and structure are shown in Table 1. The cement used in the experimental wall was composite silicate cement of P.O. 42.5 grade, the fiber was polyvinyl alcohol (PVA) imported from Japan, and the added steel mesh had a diameter of 2 mm and hole diameter of 15 mm. Laboratory testing determined that the mix ratio of plain concrete was 730 kg per cubic meter of cement, 1220 kg of sand, and 350 kg of water. ECC is a fiber reinforced cement-based composite material that exhibits high ductility under tensile and shear loads through the micromechanical design of the system. The ECC material in this paper is composed of the same mix ratio with the plain concrete and additional 4.6 kg of PVA fiber during the process of mixing.

Two field test schemes were designed. The first investigated the wave-blocking characteristics of each concrete wall. The blast wall was fixed on the ground, the DIC and overpressure test systems were installed, and 200 mg diazodinitrophenol (DDNP) explosive was used at a distance of 15 cm away from the explosion-proof wall. Due to the small experimental model, it was finally determined to be 200 mg through theoretical analysis and multiple attempts. Diazodinitrophenol , $C_6H_2N_4O_5$, pure yellow, slightly dissolved in water, with a density of 1.63 g per cubic centimeter, generally has no reaction with metal. Reasons for choosing DDNP are as follows: the diameter of detonation is small, which is suitable for small-scale model test; it has high spark sensitivity, easy for probe to touch off high-voltage electric spark detonation. This test used columnar charge, probe electric spark detonation. The overpressure was recorded at 10 cm above the ground and 10 cm behind the nine explosion-proof walls, and high-speed photography of the back-explosion surfaces was used to compare their surface strains using DIC technology. The experimental layout is shown in Figure 1.

The second test plan explored the antiexplosion characteristics of each explosion-proof wall under the same conditions. To ensure that the wall is obviously damaged, the explosive dosage was changed to 2 g DDNP and the detonation point was changed to 10 cm high on the surface of the wall, with the same columnar charge, probe electric spark detonation. High-speed photography was used to record crack propagation of the back-explosion surface and the broken situation. Because the amount of DDNP in this experiment is larger, the distance between the camera and the wall is appropriately increased to ensure that the recorded image will not be affected by flying debris and the dust and guarantee the accuracy of the test. The site layout diagram is shown in Figure 2.

2.2. Experimental Systems

2.2.1. Overpressure Test System. The overpressure test system consisted of a piezoelectric pressure sensor, a charge amplifier, an oscilloscope, and a memory. This test used a CY-YD-202 piezoelectric pressure sensor (Lianeng Electronic Technology Company of Jiangsu, China) with a sensor range of $\pm 10^4$ Pa, an accuracy of <0.05% FS, a sensitivity of 100 pC/MPa, and a resolution of 0.005% FS.

Table 1: Test conditions of explosion-proof wall models.

Test name	Distance of explosion (cm)	Thickness of wall (cm)	Height of wall (cm)	Width of wall (cm)	Reinforcement	Material
Wall 1	15	5	15	50	None	Cement mortar
Wall 2	15	5	20	50	None	Cement mortar
Wall 3	15	5	25	50	None	Cement mortar
Wall 4	15	5	15	50	None	ECC
Wall 5	15	5	20	50	None	ECC
Wall 6	15	5	25	50	None	ECC
Wall 7	15	5	15	50	Reinforcement grid	ECC
Wall 8	15	5	20	50	Reinforcement grid	ECC
Wall 9	15	5	25	50	Reinforcement grid	ECC

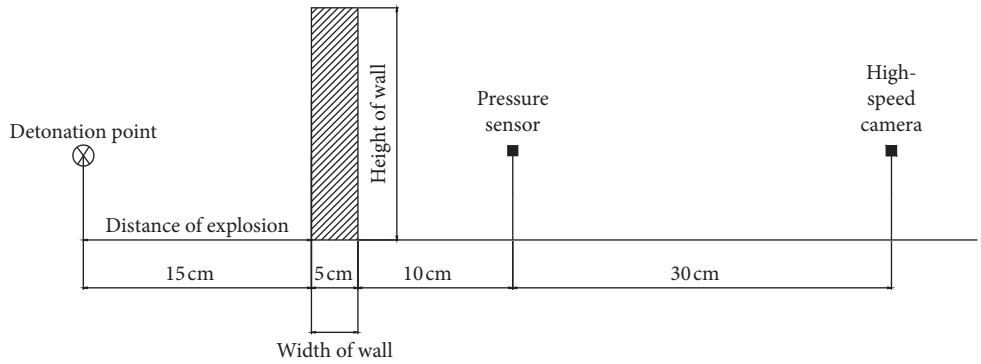

Figure 1: Layout of wave-resistance characteristics test.

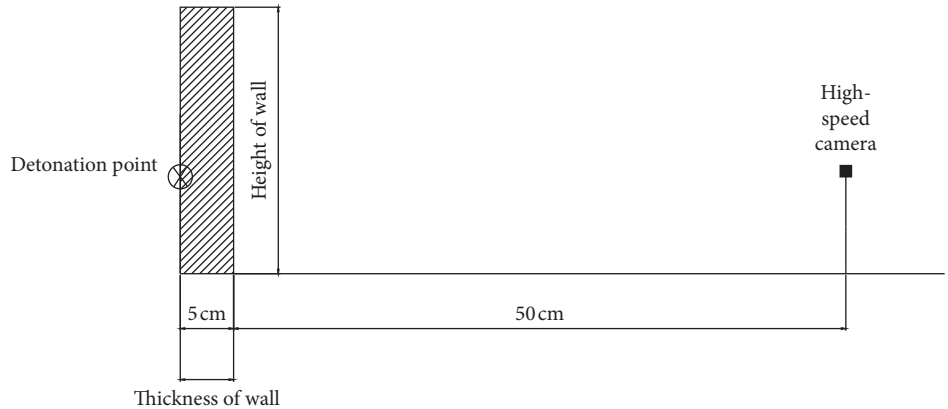

Figure 2: Layout of antiexplosion characteristics test.

2.2.2. Digital Image Correlation Test System. DIC, also known as the digital speckle correlation method, obtains digital images before and after deformation of a specimen, from which deformation information for the region of interest can be obtained through correlation calculation as shown in Figure 3. A FASTCAM SA5 high-speed camera (Photron, Japan) was used in this test. According to the optimal interval of the speckle radius of the DIC method, the radius of the artificial speckle was determined to be 2–5 mm, the selected shooting rate was 20 000 frames/s, the horizontal × vertical resolution was 832×448, and the spatial resolution is 2.2×10^{-4} mm/pixel.

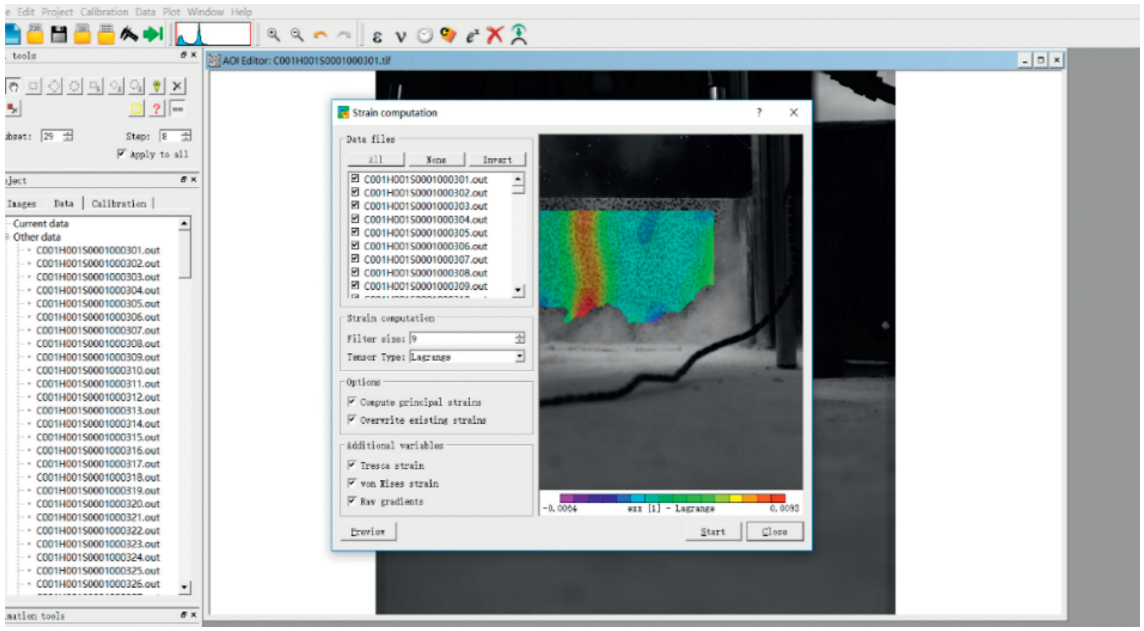

Figure 3: DIC analysis process.

3. Results and Analysis

3.1. Comparative Analysis of Overpressure Distribution. The test data were collated and the measured voltage signal converted to a pressure signal. Figure 4 shows the pressure–time curve of Wall 9. The shock-wave overpressure from a pressure sensor at a certain distance from the charging center suddenly jumped from the undisturbed zero value to the peak pressure, and the air at the rear of the wall began to expand. As time passed, the pressure began to slowly decrease until a negative pressure zone formed below the initial zero value, which met the characteristics of an explosion shock wave in the air.

Comparison of the pressure–time curves of explosion-proof walls composed of three different materials with the same height and explosion ratio showed that the three groups of walls with the same heights of 15, 20, and 25 m had the same regularity. Walls 2, 5, and 8, with a height of 20 cm, are compared as an example. Figure 5 clearly shows that the peak pressure of the concrete explosion-proof wall was the highest and the time to reach the peak pressure was the shortest. The pressure–time curves of the fiber concrete explosion-proof wall and the fiber concrete explosion-proof wall with a reinforcement grid were basically coincident, and the peak pressure was significantly lower than that of the ordinary concrete explosion-proof wall. This showed that the concrete explosion-proof wall with fiber and reinforcement grid had a stronger attenuation effect on the shock wave than the ordinary concrete explosion-proof wall.

Figure 6 shows a comparison of the pressure–time curves of three concrete blast walls with fiber and reinforcement grids of different heights. When the wall was higher, the peak pressure was smaller and the pressure reached its peak point later. This meant that a higher wall was more effective in damping a shock wave than the lower one.

According to the calculation formula for the peak overpressure of an explosion air shock wave proposed by Henrych and Abrahamson [18], the peak overpressure of the free field under the same explosion conditions can be obtained:

$$\Delta p_m = \frac{1.4072}{\overline{R}} + \frac{0.554}{\overline{R}^2} - \frac{0.0357}{\overline{R}^3} + \frac{0.000625}{\overline{R}^4}, \quad 0.05 \le \overline{R} \le 0.30; \tag{1}$$

$$\Delta p_m = \frac{0.6194}{\overline{R}} - \frac{0.033}{\overline{R}^2} - \frac{0.213}{\overline{R}^3}, \quad 0.30 \le \overline{R} \le 1.0; \tag{2}$$

$$\Delta p_m = \frac{0.066}{\overline{R}} + \frac{0.405}{\overline{R}^2} + \frac{0.329}{\overline{R}^3}, \quad 1 \le \overline{R} \le 10, \tag{3}$$

where $\overline{R} = R/\sqrt[3]{W}$ is the burst ratio (m/kg$^{1/3}$), R is the distance of explosion (m), and W is the explosive charge (kg), and the unit of Δp_m is MPa. According to the research of other scholars, the TNT equivalence of DDNP should be increased appropriately when the dose is little and the ground must absorb part of the energy [3]. The TNT equivalence of DDNP in this paper is 1.75, so $W = 0.00035$ kg and $R = 0.3$ m, so the peak value of the free-field overpressure under the same testing conditions can be calculated as 0.0421 MPa.

The overpressure ratio λ is the ratio of the overpressure peak P behind the measured explosion-proof wall to the free-field overpressure peak ΔP calculated by the empirical formula (3), from which the protection ratio η is defined:

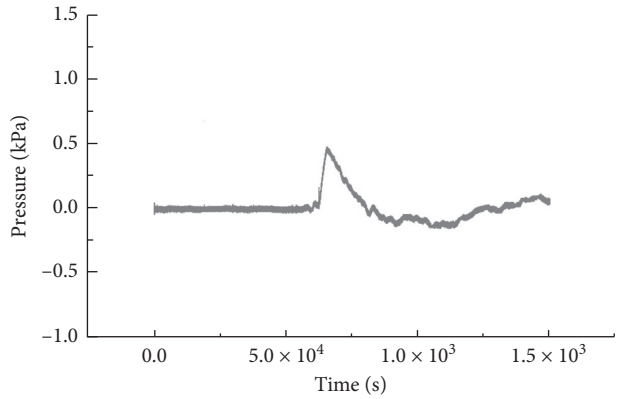

Figure 4: Overpressure–time curve of Wall 9.

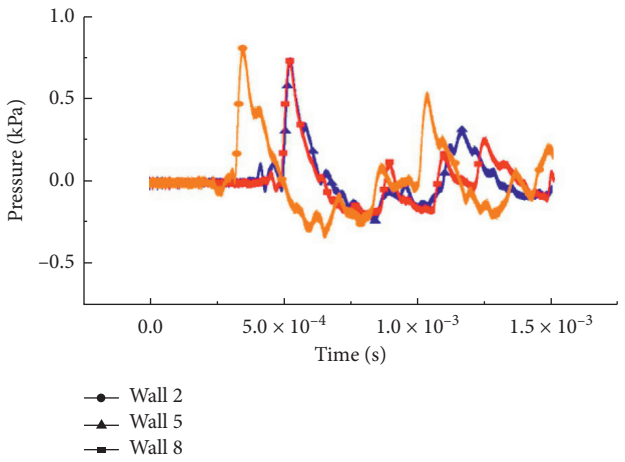

Figure 5: Comparison of overpressure–time curves of Walls 2, 5, and 8.

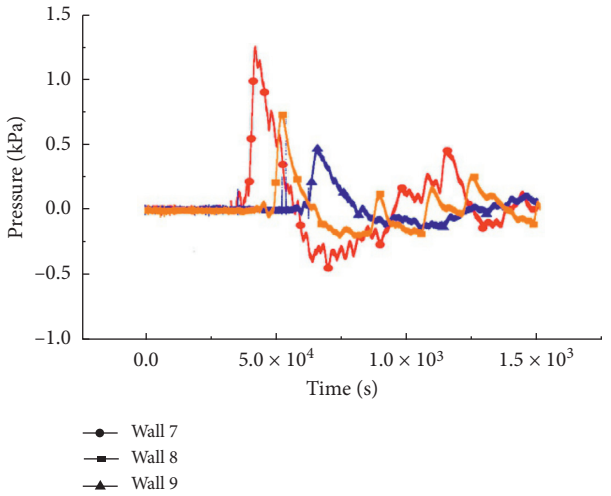

Figure 6: Comparison of overpressure–time curves of Walls 7, 8, and 9.

$$\eta = 1 - \frac{P}{\Delta P} = 1 - \lambda. \quad (4)$$

According to the measured overpressure peak, the protection ratio η of each blast wall was calculated, as presented in Table 2. The experimentally measured wall-protection values all exceeded 96%, which proved that the protective wave-eliminating effect of the explosion-proof walls was obvious under these blasting conditions. There were, however, still differences between the walls, which were in accordance with the observations mentioned above: the explosion-proof wall with ECC and a reinforcement grid had a stronger detonation energy-absorption effect than ordinary concrete, and more obviously, the walls which are higher were better than the lower ones.

3.2. Analysis of Full-Field Strain. The full-field strains of the explosion-proof walls under the blast load were obtained using VIC-2D software (Correlated Solutions Inc., (USA)) to process the blasting process, as recorded by the high-speed camera. Figure 7 shows the dynamic process of horizontal strain on the back surface of the wall, as calculated by the software. The wall had a relatively obvious strain change during the detonation process. The average horizontal strain curves of the concretes in the observation area are shown in Figure 8.

Comparison of the strain curves of Walls 2, 5, and 8, shown in Figure 8, showed that, of these three explosion-proof walls with the same height of 20 cm, Wall 2 (ordinary explosion-proof concrete) had the largest average strain under the same explosion ratio, followed by Wall 5 (explosion-proof concrete with PVA fiber), while the average strain of Wall 8 (explosion-proof concrete with PVA fiber and reinforcement grid) was lower. This showed that the addition of PVA fiber greatly reduced the tensile strain of the explosion-proof walls, which played a role in preventing tensile damage of the back-explosion surface. Addition of the reinforcement grid made the strain reduction more significant: strength of the explosion-proof wall was enhanced, so this material exhibited the best resistance to tensile failure of the back-explosion surface under the blast load.

Comparison of the strain curves of Walls 7, 8, and 9, shown in Figure 8, which all contained PVA fiber and a reinforcement grid, showed that Wall 7, with a height of 15 cm, had the largest average strain, followed by Wall 8, with a height of 20 cm. Wall 9, with a height of 25 cm, had the least variation and there was no tendency to change. This showed that, with an increase of the height of the explosion-proof wall, its ability to resist the blasting load was stronger, the overall tensile strength of the back-explosion surface was improved, and the strain was decreased, which avoided cracks.

3.3. Analysis of Destructive Form. In the second test scheme, the detonation point was moved to the surface of the wall and the amount of powder was increased to 2 g DDNP. The concrete surface fell off the surface of the explosion-proof wall and crack propagation occurred in the middle of the

Table 2: Protection ratios of various walls.

Test name	Wall 1	Wall 2	Wall 3	Wall 4	Wall 5	Wall 6	Wall 7	Wall 8	Wall 9
Protection rate	96.5%	98%	98.2	96.7%	98.3%	98.2%	96.9%	98.3%	98.8%

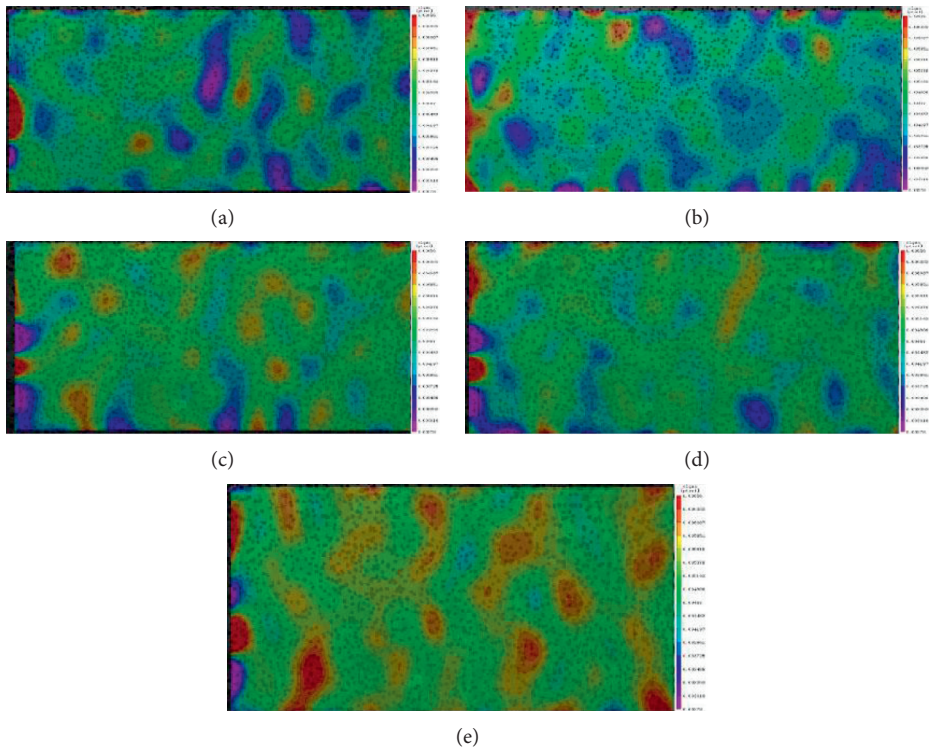

Figure 7: Dynamic changes in process of horizontal strain.

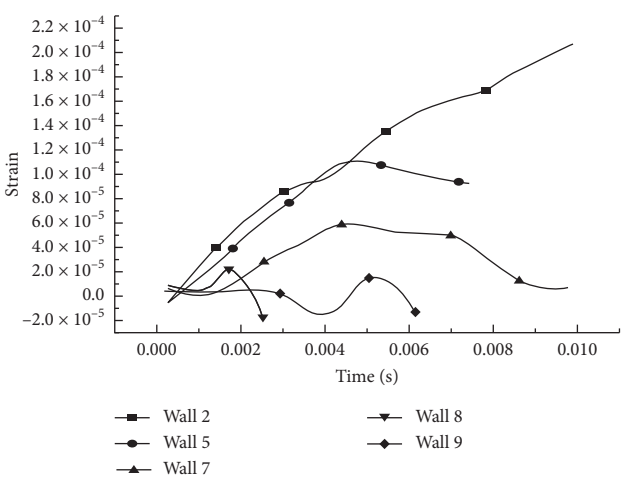

Figure 8: Strain curves of Walls 2, 5, 7, 8, and 9.

wall. The overall damage situation of each wall is shown in Figure 9.

The three common concrete explosion-proof walls in the right column in Figure 9 were seriously damaged, crack development occurred completely across the entire wall surface, and the crack width of the lower wall was

Figure 9: Overall damage of walls.

significantly larger than that of the higher wall. However, the walls with PVA fiber in the middle column only formed a small crack in one specific part, which did not cause overall damage to the wall. Cracks were not visible to the naked eye in the walls with the reinforcement grid in the left column.

Figure 10 shows breakage of the wall after damage along cracks. Compared with ordinary concrete, the section of the concrete explosion-proof wall with PVA fiber adhered to many fine fibers. Owing to the good tensile strength of PVA fiber, the tensile failure resistance of the wall back-explosion surface was significantly improved. Tensile strain on the back-explosion surface was reduced, and the detonation and energy-absorption effect of the wall improved.

(a) (b)

Figure 10: Breakage of wall along cracks.

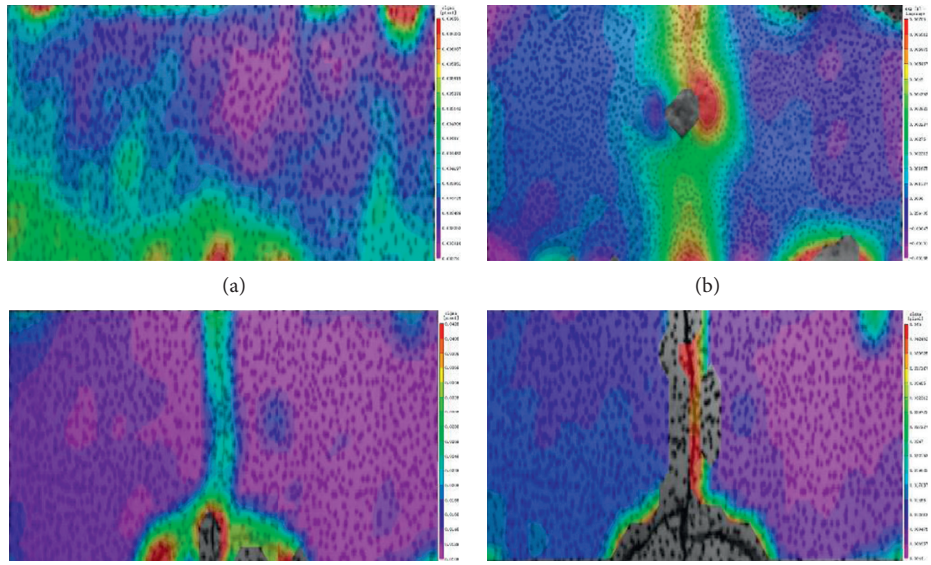

(a) (b)

(c) (d)

Figure 11: Strain cloud diagrams of failure process of normal concrete wall.

Owing to the similarity of the three groups of walls of different heights, Walls 2, 5, and 8, all with a height of 20 cm, were selected as examples to observe the strain. Figure 11 shows that the ordinary concrete explosion-proof wall produced fully developed cracks in the middle of the wall at the detonation point. The DIC method cannot continue to obtain strains of all points after cracks are generated, and therefore only strains in areas where no cracks were generated were observed in the subsequent process.

The process of destruction of Wall 5 (joined with fiber concrete) under high-speed photography is shown in Figure 12. The wall first produced a concentrated strain change at the detonation point, and then the middle part of the back-burst wall surface produced a higher tensile strain, forming a strip-shaped stress concentration zone. There were, however, no complete and obvious cracks, indicating that the addition of fiber had an obvious effect on tensile-strength improvement of the wall, preventing expansion and development of cracks.

The process of destruction of Wall 5 (joined with fiber concrete and a reinforcement grid) under high-speed photography is shown in Figure 13. A sharp change of strain first occurred from the detonation point, but because the overall intensity of the wall was high, the effects of detonation and energy absorption were obvious and tensile strength of the back-explosion surface was high. Therefore, crack development expansion or the obvious high-strain concentrated strip region observed before the formation of the middle part of the wall did not occur, and the impact was gradually absorbed by the entire wall. This showed that, under the same detonation conditions, the concrete explosion-proof wall with PVA fiber and reinforcement grid had the strongest ability to resist damage.

The strain–time curves of Walls 2, 5, and 8 before cracking are compared in Figure 14. Wall 2 (ordinary concrete) had the fastest strain response and the largest peak strain before cracking occurred, followed by Wall 5 (ECC material). Wall 8, with the fiber and the reinforcement grid, exhibited the slowest strain response and the peak strain was the lowest of the three. This showed that the change of wall material not only did have a slight impact on the delay time with respect to explosion wall damage but also greatly

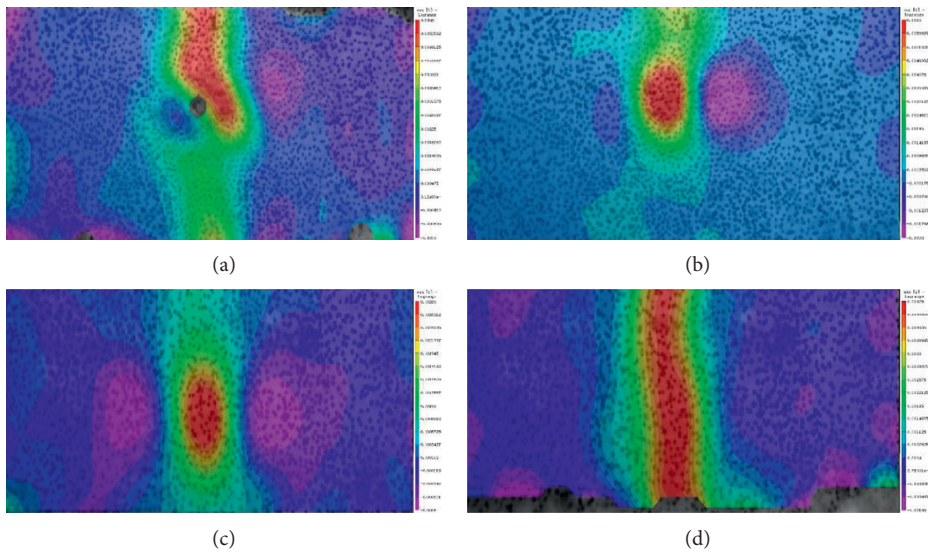

Figure 12: Strain cloud diagrams of failure process of engineered cementitious concrete wall.

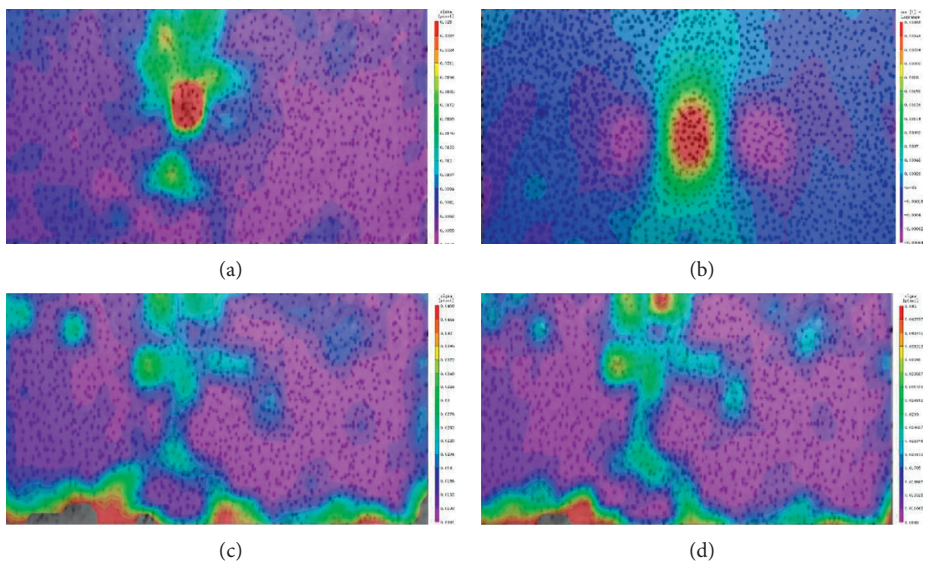

Figure 13: Strain cloud diagrams of failure process of reinforced concrete wall.

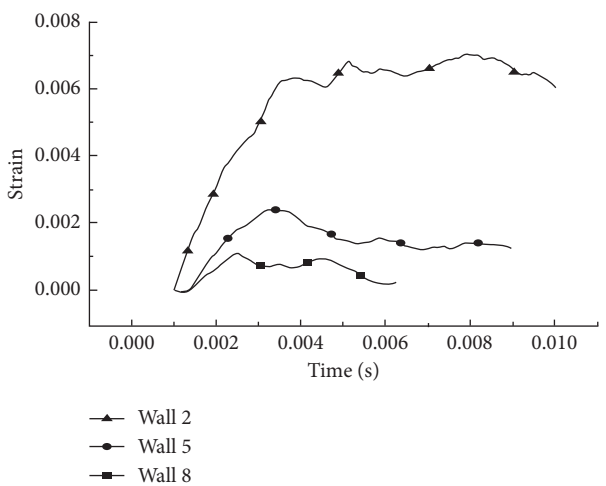

Figure 14: Comparison of strain–time curves of Walls 2, 5, and 8.

changed the strain generated before damage occurred. Under the same detonation conditions, the ECC material with the reinforcement grid had the strongest undermining effect on damage and high strain.

4. Conclusions

This study expounds the principle of an explosion shock wave acting on an explosion-proof wall and its subsequent diffraction. On-site blasting tests were conducted on self-made explosion-proof walls of different sizes and materials. DIC and overpressure test systems were used to study the detonation energy-absorption effect and dynamic response.

Experimental results showed the following:

(1) The protection of several selected explosion-proof walls, which play the role of energy absorption, all exceeded 96%. Results of on-site explosion experiments of a small-scale experimental model were in agreement with the current theory of explosion-proof walls.

(2) Under the same detonation conditions, the overpressure of the ordinary concrete explosion-proof wall was the largest, followed by the ECC explosion-proof wall with PVA fiber; the overpressure of the concrete explosion-proof wall with PVA fiber and reinforcement grid was minimal. The larger the height of the explosion-proof wall, the smaller the overpressure behind the wall. Adding PVA material and a reinforcement grid and increasing the height of the wall had obvious effects on reducing the overpressure behind the explosion-proof wall, improving its protection and strengthening its explosion-proof energy-absorption effect.

(3) For the same explosion ratio, adding PVA fiber and a reinforcement grid greatly reduced the tensile strain of the explosion-proof wall. When the explosion-proof wall was subjected to a blast load, tensile damage was not easily caused on the back surface. Crack development then occurred, resulting in overall fracture of the wall and the loss of anti-explosion ability. The height also affected the overall strain peak of the wall.

Data Availability

The data used to support the findings of this study are available from the corresponding author upon request.

Conflicts of Interest

The authors declare no conflicts of interest.

Authors' Contributions

G. Yang and W. Huang conceived and designed the experiments; W. Huang and S. Feng performed the experiments; W. Huang analyzed the data and wrote the paper.

Acknowledgments

This paper was supported by the opening project of State Key Laboratory of Explosion Science and Technology (Beijing Institute of Technology). The opening project number was KFJJ19-10M.

References

[1] K. Xu and Y. Lu, "Numerical simulatioin study of spallation in reinforced concrete plates subjected to blast loading," *International Journal of Computer and Structures*, vol. 84, no. 6, pp. 431–439, 2006.

[2] Z. G. Zhang and Z. Y. Zhang, "Numerical simulation on wave dissipating performance of rapid assembling anti-blast wall," *Chinese Journal of Blasting*, vol. 34, no. 3, pp. 157–164, 2017.

[3] X. F. Shao and H. D. Zhao, "Diffraction laws of explosion shock waves acting on portable explosion-proof walls," *Chinese Journal of Energetic Materials*, vol. 46, no. 6, pp. 6–16, 2017.

[4] Q. L. Zhang, "Effect of concrete protective wall on explosion shock wave," *Journal of Vibration and Shock*, vol. 32, no. 24, pp. 192–197, 2013.

[5] Y. L. Ma and L. J. Zhao, "Numerical simulation on different blast walls resisting air shock wave," *Chinese Journal of Blasting*, vol. 27, no. 1, pp. 36–30, 2010.

[6] H. D. Willauer, R. F. Ananth, and J. P. Arley, "Mitigation of TNT and Destex explosion effects using water mist," *International Journal of Hazardous Materials*, vol. 165, no. 1/2/3, pp. 1068–1073, 2008.

[7] T. A. Rose, P. D. Smith, and G. C. Mays, "Protection of structures against airburst using barriers of limited robustness," *Proceedings of the Institution of Civil Engineers—Structures and Buildings*, vol. 128, no. 2, pp. 167–176, 1998.

[8] K. Scherbatiuk, N. Rattanawangcharoen, and N. Charoen, "Experimental testing and numerical modeling of soil-filled concertainer walls," *Engineering Structures*, vol. 30, no. 12, pp. 3545–3554, 2008.

[9] M. Maalej, J. Zhang, S. T. Quek et al., "High-velocity impact resistance of hybrid-fiber engineered cementitious composites," in *Proceedings of the 5th International Conference on Fracture Mechanics of Concrete and Concrete Structures (FRAMCOS '04)*, pp. 1051–1058, International Association of FraMCoS, Vail, CO, USA, 2004.

[10] J. L. Zhang and Z. C. Xia, "Analysis on the explosion isolation and absorption effect of three kinds of explosion proof walls in airtight space," *Journal of Engineering Mechanics*, vol. 34, pp. 314–319, 2017.

[11] X. Z. Nian and Y. Zhang, "Analysis of transmission and diffraction effects of air shock waves upon flexible explosion-proof walls," *Journal of Engineering Mechanics*, vol. 32, no. 3, pp. 241–249, 2015.

[12] Y. Zhang and X. Z. Nian, "Mitigation effects of explosion-proof water walls and explosion-proof concrete walls on blast shock wave," *Journal of Vibration and Shock*, vol. 33, no. 18, pp. 214–220, 2014.

[13] B. Luccioni, D. Ambrosini, and R. Danesi, "Blast load assessment using hydrocodes," *Engineering Structures*, vol. 28, no. 12, pp. 1736–1744, 2006.

[14] G. K. Schleyer, M. J. Lowak, M. A. Polcyn, and G. S. Langdon, "Experimental investigation of blast wall panels under shock

pressure loading," *International Journal of Impact Engineering*, vol. 34, no. 6, pp. 1095–1118, 2007.

[15] G. S. Langdon and G. K. Schleyer, "DDeformation and failure of profiled stainless steel blast wall panels. Part III: finite element simulations and overall summary," *International Journal of Impact Engineering*, vol. 32, no. 6, pp. 988–1012, 2006.

[16] X. Q. Zhou and J. Z. Hong, "Numerical simulation of dynamic response of RC walls under blasting loading," *Journal of Disaster Prevention and Mitigation Engineering*, vol. 36, no. 1, pp. 153–158, 2016.

[17] L. Zhang and L. J. Zhang, "Dynamic response of reinforced concrete explosion-proof wall under explosion loading," *China Safety Science Journal*, vol. 18, no. 9, pp. 99–105, 2008.

[18] J. Henrych and G. R. Abrahamson, *The Dynamics of Explosion and its Use*, Elsevier Scientific Pub.Co., Amsterdam, Netherlands, 1979.